Temperature profiles derived from transverse optical shadowgraphy in ultraintense laser plasma interactions at 6×10^{20} W cm^{-2} [a)]

K. L. Lancaster,[1,b)] J. Pasley,[1,2] J. S. Green,[1] D. Batani,[3] S. Baton,[4] R. G. Evans,[1,5] L. Gizzi,[6] R. Heathcote,[1] C. Hernandez Gomez,[1] M. Koenig,[4] P. Koester,[6] A. Morace,[3] I. Musgrave,[1] P. A. Norreys,[1,5] F. Perez,[4] J. N. Waugh,[2] and N. C. Woolsey[2]
[1]*Central Laser Facility, STFC Rutherford Appleton Laboratory, Didcot OX11 0QX, United Kingdom*
[2]*Department of Physics, University of York, Heslington YO10 5DD, United Kingdom*
[3]*Dipartimento di Fisica "G. Occialini," Universita degli Studi di Milano-Bicocca, Piazza della Scienza 3, 20126 Milano, Italy*
[4]*Laboratoire pour l'Utilisation des Lasers Intenses, UMR 7605, CNRS-CEA Universite Paris VI—Ecole Polytechnique, 91128 Palaiseau, France*
[5]*Blackett Laboratory, Imperial College, Prince Consort Road, London SW7 2BZ, United Kingdom*
[6]*ILIL, CNR-IPCF, Via G. Moruzzi, 1, 56124 Pisa, Italy*

(Received 8 December 2008; accepted 21 April 2009; published online 28 May 2009)

A variety of targets with different dimensions and materials was irradiated using the VULCAN PW laser [C. N. Danson *et al.*, Nucl. Fusion **44**, S239 (2004)]. Using transverse optical shadowgraphy in conjunction with a one-dimensional radiation hydrodynamics code it was possible to determine a longitudinal temperature gradient. It was demonstrated for thick targets with a low Z substrate and a thin higher Z tracer layer at the rear that the boundary between the two materials was Rayleigh–Taylor unstable. By including a simple bubble growth model into the calculations it was possible to correct for the associated behavior with regard to temperature. The resulting temperature gradient was in good agreement with the previously published data using two different methods of determining the temperature. © *2009 American Institute of Physics*. [DOI: 10.1063/1.3133024]

I. INTRODUCTION

One of the goals of many laser plasma experiments investigating electron transport is to determine the temperature as a function of target depth. Looking at the temperature at various positions inside the solid gives an indication of the position of maximum heating and how deep significant target heating can occur. The most common way of determining temperature is to place a buried tracer layer at intervals inside the solid and use x-ray spectroscopy to determine the temperature.[1–7]

This can be difficult for several reasons. The presence of a buried layer may affect the transport—there are indications from experiments and modeling[1] that buried layers change the way electrons can propagate through the target. This means that the targets employed for transport investigations are changing the very subject of the measurement.

The second problem is that atomic physics can become quite complicated in ultraintense laser plasma interactions. Many codes used to model this physics assume Maxwellian return currents. Refluxing of electrons means that the return current has a significant hot component and this must be considered.

An alternative way to derive the temperature profile is rear surface optical shadowgraphy. Using measured rear surface expansion velocities in conjunction with a radiation hydrodynamics code it is possible to obtain a temperature gradient without using any buried layers.[8] In Ref. 8 they perform a detailed work using rear side interferometry imaging to calculate radial and longitudinal temperature profiles using a one-dimensional (1D)/two-dimensional hydrodynamics code.

In this report, rear surface expansion is measured using transverse optical shadowgraphy. The longitudinal expansion velocities can be derived from these profiles. We derive rear surface temperatures using the expansion velocities in conjunction with a 1D radiation hydrodynamics code to give temperature as a function of target thickness/electron density. We show that the radiation hydrodynamics model alone does not adequately explain the expansion behavior of the thick layered targets and it was necessary to add a simple Rayleigh–Taylor (RT) model to produce temperatures that are more in agreement with the previous work. The derived longitudinal temperature profiles are in good agreement with two other diagnostic methods employed using the same laser system. This demonstrates that a simple method of deriving longitudinal rear surface temperatures is comparable to more indirect and complicated methods.

II. EXPERIMENTAL METHOD

In this experiment a variety of targets was irradiated using the VULCAN PW laser. This report focuses mainly on thick slabs of SiO_2 and Al, 25 and 50 μm thick with 1 μm Cu layers on the rear side for Cu $K\alpha$ imaging. Small (400×400 μm^2), thin (~4 μm total) layered targets of CH/X/CH, SiO_2/X/CH, and Al/X/CH were used, where X is a tracer layer of Ni or Al.

The experiment was conducted using the VULCAN PW laser, which delivered ~440 J onto the gratings in an

[a)]Paper KI2 4, Bull. Am. Phys. Soc. **53**, 157 (2008).
[b)]Invited speaker.

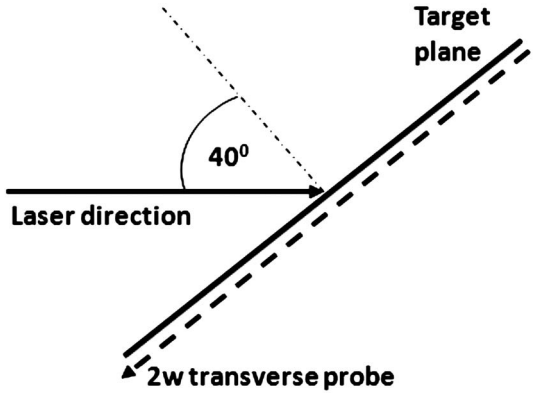

FIG. 1. Experimental layout.

~600 fs pulse. The focal spot was 6×4 μm and the intensity was $\sim6.4\times10^{20}$ W/cm^2. The laser was incident on the target at an angle of 40° (Fig. 1).

A suite of diagnostics was employed to measure the various aspects of the interaction. Optical diagnostics included transverse optical shadowgraphy and rear side optical emission imaging (specifically optical transition radiation). X-ray diagnostics included x-ray pinhole imaging, Cu $K\alpha$ imaging with a spherical crystal, and a mica crystal spectrometer.[9]

The expansion on the front and back surfaces of the target was diagnosed using a transverse optical probe. The 1.054 μm light was frequency doubled to 527 nm using a potassium dihydrogen phosphate crystal. The pulse length of the probe and main interaction beam were identical and synchronization of the beams was performed using an optical streak camera.

The shadowgraphy images were recorded at 200 ps after the interaction using an 8-bit charge coupled device (CCD) camera connected to a personal computer via image acquisition software. The magnification was 8.5 and the f number was 4.5. The resolution of the probe system was found to be ~4 μm. Interferograms were taken previously using a Normarski interferometer and a 16 bit Andor technology CCD camera. Analysis of these interferograms shows a cutoff density of 5×10^{19} cm^{-3}.

III. RESULTS AND DISCUSSION

Shadowgrams were recorded for a wide range of target types. Figures 2(a)–2(c) show typical examples of shadowgrams for thick and thin targets. Figure 2(a) is 25 μm SiO_2+1 μm Cu, Fig. 2(b) is 4 μm Al/1 μm Ni/1 μm CH, and Fig. 2(c) is 25 μm CH+1 μm Cu.

The bright feature in Fig. 2(a) corresponds to self-emission produced where the laser interacts with the target front surface. The laser is incident from the right side of the image.

The expansion velocities were calculated from the shadowgrams using the knowledge on the original target surface position and the time that shadowgram was recorded. The error in the velocities came from the combined uncertainty of the expansion position and the original target surface position.

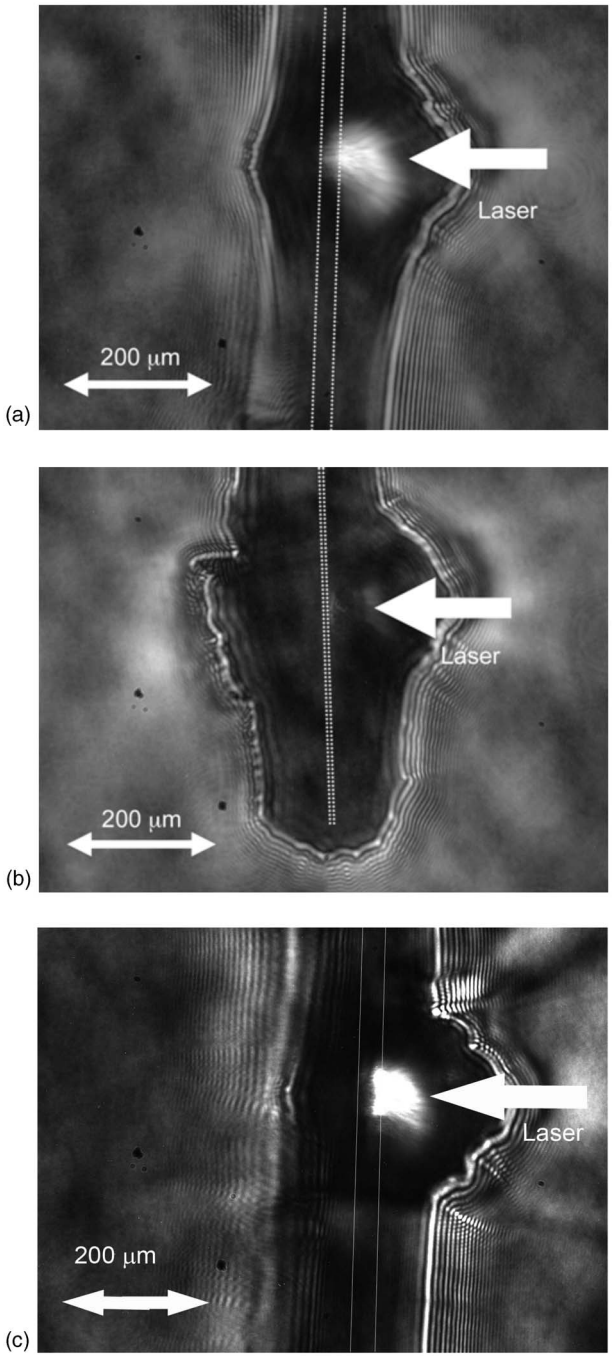

FIG. 2. (a) Shadowgraph of 25 μm SiO_2+1 μm Cu back layer taken at t_0+200 ps. (b) Shadowgraph of 4 μm Al/1 μm Ni/1 μm CH taken at t_0+200 ps. The dotted lines mark the position of the original target surfaces. (c) An example of 25 μm CH+1 μm Cu back layer taken at t_0+200 ps.

The lateral scale of the expansion for the 25 μm SiO_2 target is ~100 μm and for the thin layered target is ~200 μm. The longitudinal scale of the expansion for 25 μm SiO_2 target is ~90 μm and for the thin layered target is ~265 μm. We know that the images were taken at t_0+200 ps and so the expansion velocities (depending on the thickness) were in the range of 2×10^7–1×10^8 cm/s.

The next step in the analysis was to use the experimentally derived expansion velocities in conjunction with a radiation hydrodynamics model to derive a temperature gradi-

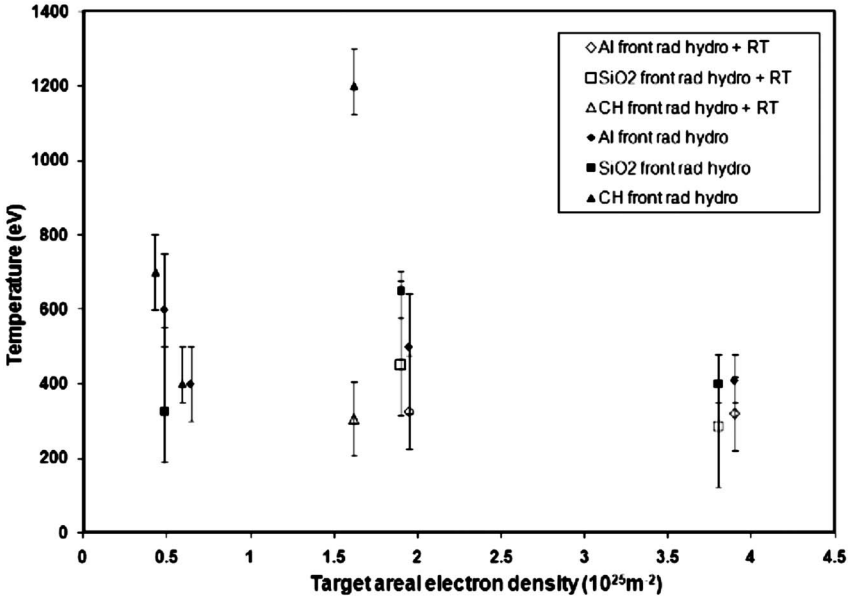

FIG. 3. Comparison of rear surface temperatures derived from expansion velocities (measured from shadowgraphy) using HYADES alone (open shapes) and HYADES with RT model (black shapes) models.

ent. The trajectory of the imaged density contour (from the shadowgraphy) is matched to the predictions of radiation hydrodynamics simulations to obtain an estimate of the bulk temperature attained in each target. HYADES (Ref. 10) is a 1D Lagrangian radiation hydrodynamics simulation code with a multigroup radiation diffusion model and a flux limited diffusion model of electron conduction.

In these simulations, an average atom local thermodynamic equilibrium ionization model and tabulated SESAME equation of state data are employed. The targets are given an initial temperature to mimic the heating of the short pulse and HYADES then models the cooling and expansion over time. This approach is considered reasonable since the heating is essentially instantaneous with respect to hydrodynamic time scales. Temperature is iterated to match the observed rear surface trajectory.

Further simulations are performed to match the associated minimum and maximum excursions as dictated by the experimental error bars as part of the error analysis for temperature. The thicker targets fielded are expected to be susceptible to the RT fluid instability.[11,12] The Cu back layer will cool rapidly by radiative emission and thereafter be pushed by the less dense lower-Z layer beneath it. The interface between the two regions will therefore be RT unstable since the gradient of the pressure is of the opposite sign to the gradient of the density at the boundary. For instance, 50 ps after the interaction in the CH–Cu target, the radiation hydrodynamics calculations suggest that the pressure will fall from a value of ~ 75 Mbar in the CH to ~ 25 Mbar in the Cu over a distance of ~ 1.5 μm, while the density rises in this same region from ~ 0.8 to ~ 6 g/cm^2. Under such conditions, the RT instability will inevitably grow from any initial small-scale nonuniformity in the boundary region (such as will inevitably exist after target manufacture). A simple bubble growth model[13] of the form $h_b = \alpha A_t a t^2$, in which h_b is the bubble height, A_t is the Atwood number, and α is a scaling constant, is used to estimate the time at which bubbles of the lower-Z material will penetrate through the 1 μm thick Cu back layer.

In such a model the value of α is found from the last experiments to be in the range of 0.04–0.07 (see Ref. 14); the value of this parameter is therefore assumed to lie in this range and the effect of the associated uncertainty is incorporated in the error analysis for temperature.

In evaluating the temperature, the copper rear surface layer in the simulation is effectively replaced by the underlying material at the time at which the bubbles are expected to penetrate. The value of acceleration a, which must be inserted into the growth model to yield the penetration time, is estimated on the basis of the experimental results. This is considered reasonable since the expansion of the lighter fluid, once present at the rear surface of the target, will exceed that of the copper.

Figure 3 shows the two methods of determining the rear surface temperature plotted against the target areal electron density. This value is used instead of thickness to make it easier to compare multiple-material targets. The targets are identified in the legend by the material that the laser interacts with, but the areal density plotted is that of the whole target including all layers.

The colored shapes are the simulations without the RT model included. The temperatures for the thick targets with Cu layers on the rear surface (i.e., targets greater than 1.5×10^{25} m^{-2}) produced temperatures that fall outside the upper bounds of previous experimental and theoretical data.[1,7] This is especially evident in the case of CH with a Cu layer, which is a factor of $\sim 2-3$ higher. The thin target data are in reasonable agreement however.

A simple model for the RT instability was added (as described earlier in this section) due to the rapid radiative cooling of the copper compared to the lower Z base material. The rear surface of the thin targets was not expected to be RT unstable as it comprises uncoated plastic. Note that in the RT unstable targets it is not expected that any nonuniformity will

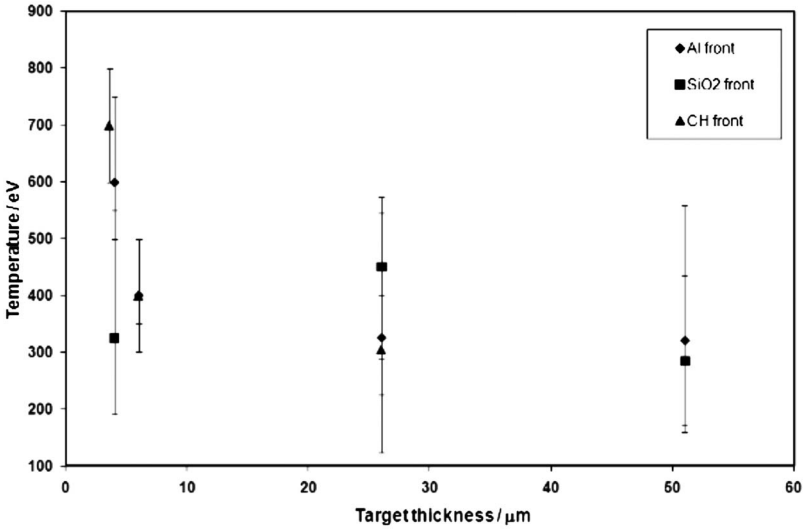

FIG. 4. Temperatures from HYADES (with RT model for thick targets with Cu layer) as a function of target thickness.

be observed as a consequence of the instability in the side-on imaging. Growth will be three-dimensional multimodal and is expected to be dominated by wavelengths below those resolvable by the imager. Figure 2(c) shows that no visible ripples due to RT are seen in the CH target shadowgram.

Simulations for the thick targets with Cu layers were repeated using this technique. The open shapes in Fig. 3 represent the radiation hydrodynamic calculations with the RT model included.

Temperatures in the thick targets were reduced to a more reasonable level compared to experimental data/hybrid models, most dramatically the case of CH coated with 1 μm Cu. This demonstrates that failure to combine the RT model with the hydrodynamic calculations for potentially RT unstable boundaries results in the overprediction of rear surface temperature.

Figure 4 shows a plot of temperature at the rear surface as a function of total target thickness. The curves are identified by the material onto which the laser is incident. The temperature derived from the radiation hydrodynamics code reaches ~700 eV at 3.5 μm targets down to a value of ~300 eV at 50 μm. The plastic targets appear to attain the highest temperatures. The temperatures for CH and Al drop to ~400 eV within 2.4 μm, a rapid fall with increasing target thickness.

The temperature gradient derived from using HYADES in conjunction with the RT model shows reasonable agreement with the previously published VULCAN PW data both from Refs. 1 and 7. The observed double gradient described in Ref. 7 is clearly visible in our data with the rapid falloff of temperature up to $1-1.5\times10^{25}$ m^{-2} after which the falloff in temperature becomes much slower. As stated in Ref. 7, the higher temperatures in thinner targets are likely due to refluxing of hot electrons, and the sharp falloff is due to the effect of refluxing dropping off as the target thickness is increased.

IV. CONCLUSIONS

We have shown that it is possible to use a relatively simple method of shadowgraphy in conjunction with a 1D radiation hydrodynamics model to derive a temperature profile for various types of layered target. Where present, the interface between the lower-Z material and the copper was RT unstable, due to the faster radiative cooling of the copper resulting in a steep pressure gradient at the interface. A radiation hydrodynamics model used in combination with a simple model for RT growth produced temperatures more closely resembling the previously measured temperatures from the same system using x-ray spectroscopy and time resolved rear surface optical emission. From this we can conclude that the model is reasonable and provides a more direct/simple way of deducing rear surface temperature gradients in a variety of circumstances.

ACKNOWLEDGMENTS

The author would like to acknowledge the Vulcan laser staff, engineering staff, and target preparatory staff for all their hard work and assistance in making this experiment possible.

[1] R. G. Evans, E. L. Clark, R. T. Eagleton, A. M. Dunne, R. D. Edwards, W. J. Garbett, T. J. Goldsack, S. James, C. C. Smith, B. R. Thomas, R. Clarke, D. Neely, and S. J. Rose, Appl. Phys. Lett. **86**, 191505 (2005).
[2] J. Koch, M. H. Key, R. R. Freeman, S. P. Hatchett, R. W. Lee, D. Pennington, R. B. Stephens, and M. Tabak, Phys. Rev. E **65**, 016410 (2001).
[3] F. Pisani, A. Bernardinello, D. Batani, A. Antonicci, E. Martinolli, M. Koenig, L. Gremillet, F. Amiranoff, S. Baton, J. Davies, T. Hall, D. Scott, P. Norreys, A. Djaoui, C. Rousseaux, P. Fews, H. Bandulet, and H. Pepin, Phys. Rev. E **62**, R5927 (2000).
[4] U. Andiel, K. Eidman, F. Pisani, K. Witte, I. Uschmann, O. Wehrhan, and E. Forster, Rev. Sci. Instrum. **74**, 2369 (2003).
[5] E. Martinolli, M. Koenig, S. D. Baton, J. J. Santos, F. Amiranoff, D. Batani, E. Perelli-Cippo, F. Scianitti, L. Gremillet, R. Melizzi, A. Decoster, C. Rousseaux, T. A. Hall, M. H. Key, R. Snavely, A. J. Mackinnon, R. R. Freeman, J. A. King, R. Stephens, D. Neely, and R. J. Clarke, Phys. Rev. E **73**, 046402 (2006).
[6] K. U. Akli, S. B. Hansen, A. J. Kemp, R. R. Freeman, F. N. Beg, D. C.

Clark, S. Chen, D. Hey, S. P. Hatchett, K. Highbarger, E. Giraldez, J. S. Green, G. Gregori, K. L. Lancaster, T. Ma, A. J. MacKinnon, P. Norreys, N. Patel, J. Pasley, C. Shearer, R. B. Stephens, C. Stoeckl, M. Storm, W. Theobald, L. D. Van Woerkom, R. Weber, and M. H. Key, Phys. Rev. Lett. **100**, 165002 (2008).
[7]M. Nakatsutsumi, J. R. Davies, R. Kodama, J. S. Green, K. L. Lancaster, K. U. Akli, F. N. Beg, S. N. Chen, D. Clark, R. R. Freeman, C. D. Gregory, H. Habara, R. Heathcote, D. S. Hey, K. Highbarger, P. Jaanimagi, M. H. Key, K. Krushelnick, T. Ma, A. MacPhee, A. J. Mackinnon, H. Nakamura, R. B. Stephens, M. Storm, M. Tampo, W. Theobald, L. Van Woerkem, R. L. Weber, M. S. Wei, N. C. Woolsey, and P. A. Norreys, New J. Phys. **10**, 043046 (2008).
[8]G. Malka, Ph. Nicolai, E. Brambrink, J. J. Santos, M. M. Aleonard, K. Amthor, P. Audbert, J. Breil, G. Claverie, F. Gobet, F. Hannachi, V. Meot, P. Morel, J. N. Scheurer, M. Tarisien, and V. Tikhonchuck, Phys. Rev. E **77**, 026408 (2008).
[9]P. Köster, K. Akli, D. Batani, S. Baton, R. G. Evans, A. Giulietti, D. Giulietti, L. A. Gizzi, J. S. Green, M. Koenig, L. Labate, A. Morace, P. Norreys, F. Perez, J. Waugh, N. Woolsey, and K. L. Lancaster, Plasma Phys. Controlled Fusion **51**, 014007 (2009).
[10]HYADES is a commercial product of Cascade Applied Sciences, larsen@casinc.com.
[11]L. Rayleigh, Proc. London Math. Soc. **14**, 170 (1883).
[12]G. I. Taylor, Proc. R. Soc. London, Ser. A **201**, 192 (1950).
[13]C. L. Gardner, J. Glimm, O. McBryan, R. Menikoff, D. H. Sharop, and O. Zhang, Phys. Fluids **31**, 447 (1988).
[14]S. Atzeni and J. Meyer-ter-vehn, *The Physics of Inertial Fusion* (Clarendon, Oxford, 2004).